Impact Response Of Concretefilled Steel Tubular Members (CFST) Using Different Types Of Concrete Filling.

Anwar Badawy,Hanan H. Eltobgy, Emad Darwish, Mahmoud Morgan

Abstract :In this paper, experimental and numerical studies were carried out to investigate the performance of normal concrete (N.C), polypropylene fiber concrete (P.F.C), steel fiber concrete (S.F.C), and high strength concrete (H.S.C) filled steel tubes under lateral impact loading.A total of eight specimenswere tested divided into two groups, four specimens for each for the four types of concrete. The first group the specimen'sdimension were 114.3 mm diameter and 4 mm thickness, and the other group with dimension of 88 mm diameter and 4 mm thickness. The average cubic strength for all concrete was Fcu=45 N/mm^2, except for the high strength concrete wasFcu=70 N/mm^2. The specimens were tested using drop-weight impact test rigs with fixed- sliding boundary conditions at ends.The parameters studied were types of concrete,the length to diameter aspect ratio, and the confinement factor effect.The failure mode and local damages of the specimens were thoroughly investigated.A finite element analysis (FEA) model was also performed to simulatethe performance of (CFST) members against lateral impact loading and the predicted resultsfrom the FEA model were validated with the corresponding experimental results.Wide range analyses of the (CFST) specimen'sresponse against impact loading were then carried out using the validated FE models to examine the deformation and the energy dissipation of each concrete type.The main findings are as follows: (1) The lowest value for the total impact energy and maximum dynamic displacement were recorded for all specimens filled with polypropylene concrete specimens. While the maximum recovery energy was observed for the same specimens in group (I). (2) Nearly the same value for the total impact energy and maximum dynamic displacement were recorded for the specimens filled with ordinary concrete and high strength concrete, which mean that no benefit was gained form increasing the concrete strength.On the other hand, it may have triggered brittle failure for the concrete core. (3) high strength concrete specimens has The lowest values of constraining factor (ξ) , which behave in the most brittle failure pattern. so, Ductility of the tested specimens increase with the constraining factor (ξ).

Index Terms: Impact load, concrete filled steel tube CFST, Steel fiber concrete, propylene fiber concrete, high strength concrete.

1 INTRODUCTION

THe concrete filled steel tubes (CFSTs) are used increasingly in modern construction project [1-3] as it provide more advantages than the conventional steel membersand theordinary reinforced concretemembers. The steel tube constrains its core concrete, thus and improve the plastic deformation capability of core concrete and delay the longitudinal cracking of concrete under compression; on the other hand, the concrete core can delay or preventlocal buckling of steel tube. As a result, CFST has better ductility and toughness, higher bearing capacity, high speed of construction work resulting from the omission of formwork and reinforcing bars , low structural costs, conservation of the environment [4, 5], and better fire resistance compared with single steel tube or core concrete, that leads to a reduction in fireproof materials usage [6]. CFST members may be subjected to accidental explosion or transverse impact loads during theirservice lifetime. For examples, high risingbuildings could be attacked byan aircraft, or falling loads [7, 8], bridge columns could be impacted bya vehicle or boat.The failure of such vital structural membersmay lead to progressive collapse and further disproportionate collapse. Therefore,attention should be given to study and understand the elastic–plastic behavior of a column under high impact loading, especially to CFST columns due to the high bearing capacity they provide.

The behaviour of(CFSTs) subjected to lateral impact loads has been theoretically and experimentally investigatedin numerousresearches. An experimental and analyticalstudy was conducted by Bambacha et al. [9]on steel hollow sections and CFST beams subjected to transverseimpact loads. They proposed a design procedure for the (CFSTs) based on an elastic-plastic theoretical model. Yong et al.[10] conducted an Experimental studiesto investigate the effect of impact load on specimens filled with normal aggregate concrete steel tube (NACFST) and recycled aggregate (RACFST). The result shown that the square RACFST specimens have an almost equivalent lateral impact resistance as normal NACFST specimens.Al-HusainY et al [11] investigated the impact response of recycled aggregate concrete infilled steel tube columns strengthened with CFRP. They found that both the RACFST and NACFST specimenshad a similar deformation modeunder impact load, and the additional confinement of the CFRP reduced the global displacement for both types of specimens.Qu et al.[12] developed a simplified analytical model for circularCFST columns with fixed-simple supported ends subjected to lateral impact loading based on experimental results and numerical simulation using LS-DYNA. the proposed model could well predict the maximumdeflection of CFST specimen under lateral impacts. An experimental and numerical study on the Lateral impact response of rectangular hollow and partially concrete-filled steel tubular columns was conducted by Ai-Zhu. et. [13]. They concluded that the performance of partially concrete-filled steel tubular (PCFST) specimensis better than the performance of the rectangular hollow steel tubular (RHST) specimens.Deng et al. [14]investigated the failure modes and local damages of the nine simply

- *Professor of Steel Structures and Bridges, Civil Engineering Department, Faculty of Engineering at Shoubra, Benha University, Email: Anwar.Badawy@feng.bu.edu.eg*
- *Associate Professor of Structural Engineering, Civil Engineering Department Faculty of Engineering at ShoubraBenha University, Email: hanan.altobgy@feng.bu.edu.eg*
- *Lecturer of Structure Engineering, Civil Eng. Department, Faculty of Engineering, Shoubra, Benha University, Cairo, Egypt, Email: emad.darwish@feng.bu.edu.eg*
- *Assistant Lecturer of Structure Engineering, Civil Eng. Department, Faculty of Engineering, Shoubra, Benha University*, Cairo, Egypt, Email: mahmoud.morgan@feng.bu.edu.eg

supported CFST, two steel post-tensioned CFST and one steel fiber-reinforced concrete filled tube under lateral impacts. The height and the weight of the drop-hammer were varied to cause failure in some test specimens.Failure in the steel tubes was tensile facture or rupture along the circumference. Concrete corecrushed under compression and cracked under tensionin the impact area. The use of prestressing strands and steel fibers significantly restrained the concrete tension cracks. Despite numerous previous researches on the structural behaviour of the CFST columns under impact loading, only limited numbers of research have been conducted on the impact behavior of steel tube filled with various types of concrete such as steel fiber concrete, polypropylene fiber concrete or high strength concrete. Therefore, in this study we aim to investigate the performance of CFST members filled with different types of concrete under the effect of lateral impact load. Also, the effect of aspect ratio (L /D) and the confinement factor (ξ) on the performance of concrete filled steel tube is investigated. This research has triplet purposes; First, to conduct a series of new experimental tests on eight circular CFST specimens under lateral impact load divided into two groups with different diameter 114mm and 88 mm but same wall thickness of 4 mm. the testing parameters are the concrete type, the pipe diameter, as well as the confinement factor. Second, to study the time history of the impact forces, and the global deformation, as well as the absorption energy for each specimen based on the testing results. Third, to provide a finite element analysis (FEA) model to predict the response of (CFST) members under impact loads,using Abaqus software applications. the accuracy of the (FEA) model was validated by comparison with the experimental results.

2 EXPERIMENTAL PROGRAM

2.1 SPECIMEN PREPARATION

The experimental testes were carried out on eight circular CFST members. Specimen's outer sectional diameter (D) was 114.3 mm and 89 for group (I) & group (II) respectively, with effective length of 1200 mm and overall length1500mm. the steel tube wall thickness $t_s$for all specimens was 4mm.The boundary conditions of the specimens were fixed from one end and sliding for the other end.

Material PROPERTIES

A locally supplied Materials were used in this study such as mild steel for tube, cement, aggregate, steel fibers, and propylene fiber as shown in Fig. 3***FIG. 3***. These materials were tested in accordance with the relevant EN and BS standards. Ordinary Portland cement CEM I/42.5N complying with the requirements of British Standard BS EN 197-1 [15] was used in the preparation of the concrete mix. Normal coarse aggregate(NA) was used with maximum size of 10 mm, graded according to the British Standard BS 882 [16] This size was selected in proportion with the specimen's diameter. Normal silicious sand was used as fine aggregate in the concrete mix. The concrete was poured in layers and compacted with vibrator in the steel tube. The mean cube compressive strength of theN.C, PP.C, and SF.C concrete was designed with approximately 45 MPa at 28-day. While, for HS.C was approximately 70 MPa. The concrete mixing, pouring, and curing, as well as theconcretes cubes and cylinders used to obtain the cube's compressive strength (Fcu) and elastic modulus (Ec) are shown in Fig. 4. A standard tensile coupon test was conducted on three samples from the two types of steel tube with the standard dimensions. The average values of the yield strength, ultimate strength and the elongation are 326N/mm^2, 460 N/mm^2, 23% respectively. The modulus of elasticity (Es) for specimens is 2.01×10^5 N/mm^2.

TABLE 1. represent thedetailed information of each specimen. Concrete's mix design along with the properties of fresh concrete are annotated in **Reference source not found.**. The initial impact energy induced for the first and second group of specimens was 4900 J ± 150 J, and 3800 J ± 50 J respectively. depending on the total drop hammer mass (m) of 390kg.The carrying capacity of CFST specimens was determined based on their mechanical property and the section physical dimension.

Table **2.**The cubic strength of all concrete types was (Fcu=45 N/mm2) except for high strength concrete was (Fcu=70 N/mm2).The abbreviations, "N.C", "P.F.C", "S.F.C" or "H.S.C" are used to describe the concrete type in each specimen, which mean normal concrete, propylene fiber concrete, steel fiber concrete or high strength concrete respectively. High speed camera was used to record the marked point that fixed on the drop hammer during falling, afterwards this record was used to calculate the initial impact velocity immediately before collision between drop hammer along with the CFST specimens as shown inFig. 1&Fig. 2. The initial impact velocity (Vo) was 5.03m/sec for group (I) of specimens and 4.45 m/sec for group (II). During each test, aload cell of 800kn capacity was used to measure the force-time history, and the global displacement were recorded by LVDT. The total impact energy (W) was calculated based on the area under curve of impact load vs total displacement graph as shown in **Error!**

2.2 MATERIAL PROPERTIES

A locally supplied Materials were used in this study such as mild steel for tube, cement, aggregate, steel fibers, and propylene fiber as shown in Fig. 3***FIG. 3***. These materials were tested in accordance with the relevant EN and BS standards. Ordinary Portland cement CEM I/42.5N complying with the requirements of British Standard BS EN 197-1 [15] was used in the preparation of the concrete mix. Normal coarse aggregate(NA) was used with maximum size of 10 mm, graded according to the British Standard BS 882 [16] This size was selected in proportion with the specimen's diameter. Normal silicious sand was used as fine aggregate in the concrete mix. The concrete was

poured in layers and compacted with vibrator in the steel tube. The mean cube compressive strength of theN.C, PP.C, and SF.C concrete was designed with approximately 45 MPa at 28-day. While, for HS.C was approximately 70 MPa. The concrete mixing, pouring, and curing, as well as theconcretes cubes and cylinders used to obtain the cube's compressive strength (Fcu) and elastic modulus (Ec) are shown in Fig. 4. A standard tensile coupon test was conducted on three samples from the two types of steel tube with the standard dimensions. The average values of the yield strength, ultimate strength and the elongation are 326N/mm^2, 460 N/mm^2, 23% respectively. The modulus of elasticity (Es) for specimens is 2.01×10^5 N/mm^2.

TABLE 1.

SPECIMENS PROPERTIES.

	SPEC. ID	Pipe Type	Conc. Type FCU(MPA)	ζ	$t_{d.e}$ (ms)	$P_{K.e}$ (KN)	$P_{s.e}$ (KN)	$U_{mm,\ e}$ (mm)	U_{mr} (mm)	W (J)	$W_{Recovery}$ (J)	Concrete failure
Pipe 114.3*4MM Clear Length =1200MM												
Group (I)	SP(1)	114.3*4	N.C. FCU=450	1.75	32.6	237	79	64	56	5056	-261	A
	SP(3)	114.3*4	P.F.C Fcu =450	1.75	29.9	214	96	59	48	4801	-364	B
	SP(5)	114.3*4	S.F.C Fcu =450	1.75	32.9	284	84	63	53	5135	-210	A
	SP(7)	114.3*4	H.S.C Fcu=700	1.12	35.3	268	79	65	55	4929	-263	B
Group (II)	SP(9)	89*4	N.C. FCU=450	2.30	42.5	174	57	74	64	3864	-100	B
	SP(10)	89*4	P.F.C Fcu =450	2.30	45.2	154	54	77.3	69	3665	-10	A + B
	SP(11)	89*4	S.F.C Fcu =450	2.30	47.2	188	52	84	77	3975	-72	A
	SP(12)	89*4	H.S.C Fcu=700	1.50	46.0	195	52	80	71	3741	-121	B

A: tensile cracks at tension side, B: facture of concrete core.

TABLE 2.

MIX DESIGN AND PROPERTIES OF FRESH CONCRETE.

Type	Cement (kg/m3)	Sand (kg/m3)	Aggregate (kg/m3)	Water (kg/m3)	Admi.Type (ltr)		S .F. (kg/m3)	P.F. (kg/m3)	Silica fume	Slump (mm)	Fcu (MPA)	Ec (N/mm2)
					PC	F						
N.C	460	650	1110	185	0	5.5	-	-	-	150	44.5	29818
P.F.C	460	650	1110	185	0	5.5	-	0.9	-	130	46.1	30349
S.F.C	460	650	1080	185	0	5.5	30	-	-	120	46.8	30579
H.S.C	400	700	1100	165	9.5	0	-	-	40	260	70.5	36532

(P.F.) Polypropylene Fiber, (S.F) Steel Fiber. (PC) polycarboxylate. (F) supper plasticizer

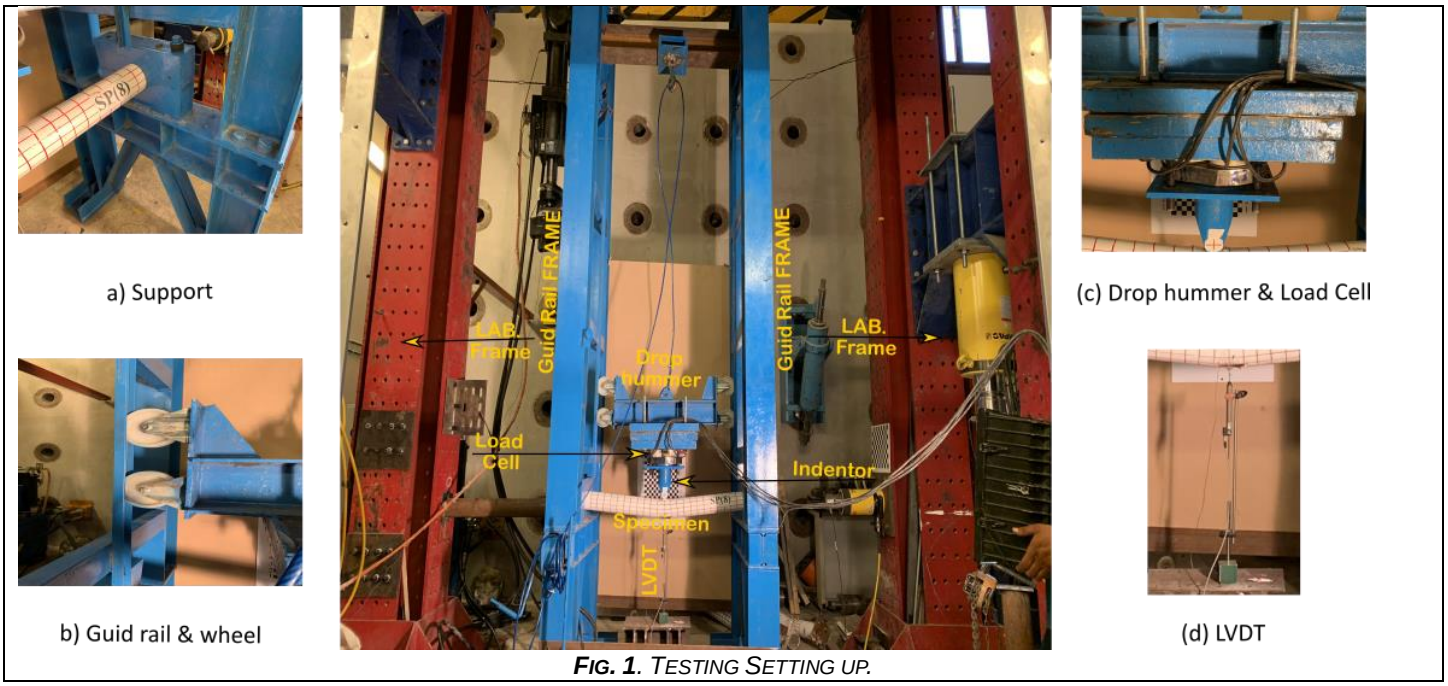

FIG. 1. TESTING SETTING UP.

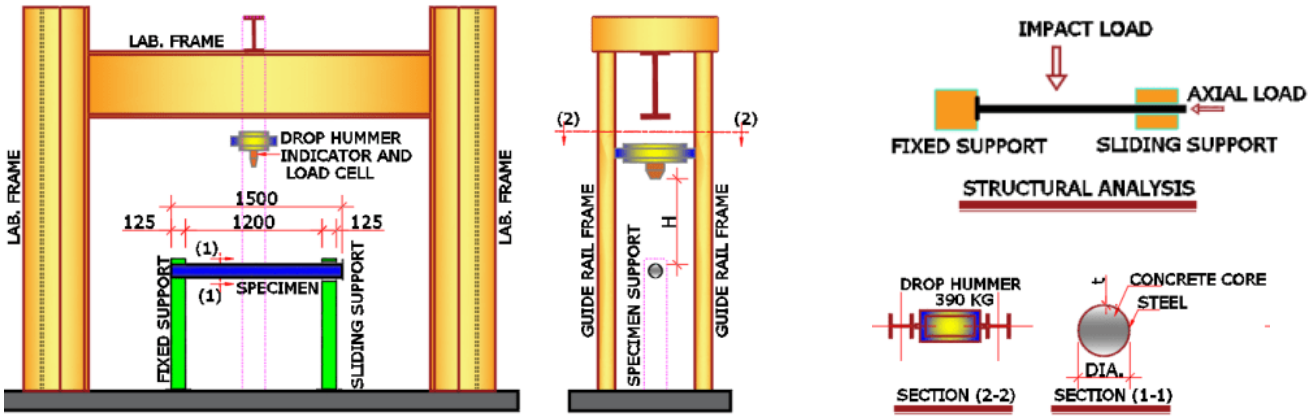

***FIG. 2**. SCHEMATIC VIEW FOR TESTING SETTING UP.*

(a) Coarse Aggragate (b) Steel Fiber (c) Polypropylene Fiber

***FIG. 3**. THE CONCRETE MIX MATERIALS.*

a) Mixing b) Curing c) Con. Cylinders

***FIG. 4**. CONCRETE MIXING & CURING, AND CONCRETE CYLINDERS& CUBE TO BE TASTED LATER.*

2.3 TESTING METHOD

The CFST specimens was placed in the testing device equipped with fixed-sliding end supports. The specimens were tested against dynamic lateral impact load, as shown inFig. 1&Fig. 2. the impact height (H) was 170 cm & 110 cm for group one and two, respectively. The mass of the drop hammer was 390 kg. The hammer is formed from solid steel cylinder with indenter having rigid flat square cross section of 30 mm×80 mm. A load cell of 800kn capacity wasassembled in the drop hummer between the weight and the impactor to record the force–time data during the test. The drop hammer was released from the design height to impose nearly the same impact load at the mid-span of the specimens for each group. The load cell recorded the time-history curves of the impact force and, the Linear Voltage Differential Transformer (LVDT) were used to record the time-history curves of displacement.

3 EXPERIMENTAL RESULTS AND DISCUSSIONS

The response of CFST specimens under lateral impact loading was initially represented in a combination of local deformation and global bending as shown in

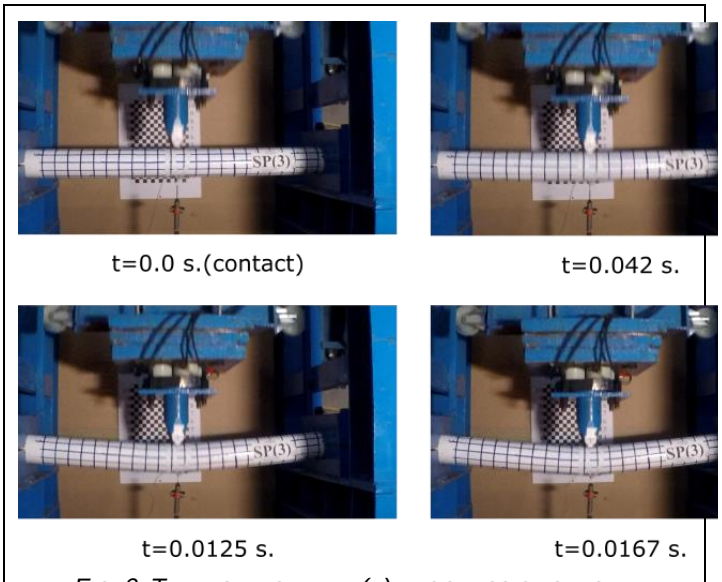

FIG. 6. THE DISPLACEMENT (U) PROGRESS OF SPECIMEN SP(3).

, followed by quick increase in the lateral displacement. The failure started from the initial contact between impact head and the specimens and finished at the same time the impact load basically reached a stable stage as shown in Fig. 6. The finalfailure pattern of the CFST specimens is generally characterized by a "V" shape of the specimens within mid-span .The responses of the tested specimens showed a plastic failure mechanism due to bending, and the plastic hinges is formed at location of impact area in the mid-span. The displacement (u) progress of specimen SP (3) is shown in **Error! Reference source not found.**. with 0.042 s interval till reaching the maximum dynamic displacement ($u_{mm,\ e}$). The most important recordeddata during the impact tests are the impact load(P) time history of specimen, and the related displacement history applied on the specimen. The typicaltime history of specimen's impact loads is represented in

Fig. *7*. The impact load (P) versus time (t) history curve is generally characterized by three stages, namely oscillation stage (point O to A),stabilization stage (point A to B) and attenuation stage (point B to C) [10]. The stabilization stage (points A and B) is determined based on variation range of P is less than 5 kN within 1 ms. After point A, a sudden change occurred to the slope of P–t curve and started from point B till the end of test. In the oscillation stage, a maximum value of impact load is reached followed by fastdecays within a short time. In the stabilization stage the impact load is generally constant. Finally, in the attenuation stage the impact load had been gradually reduced to zero when the impact energy was mostly dissipated. The maximum force recorded in tests is called the experimental peak ofimpact load ($P_{k,e}$) , and the average impact force within the first 15 ms in the stabilization stage is calledas the plateau of impact load ($P_{s,e}$) as the fluctuation of P small during this period. The time history of impact load (P) for all specimens are shown in

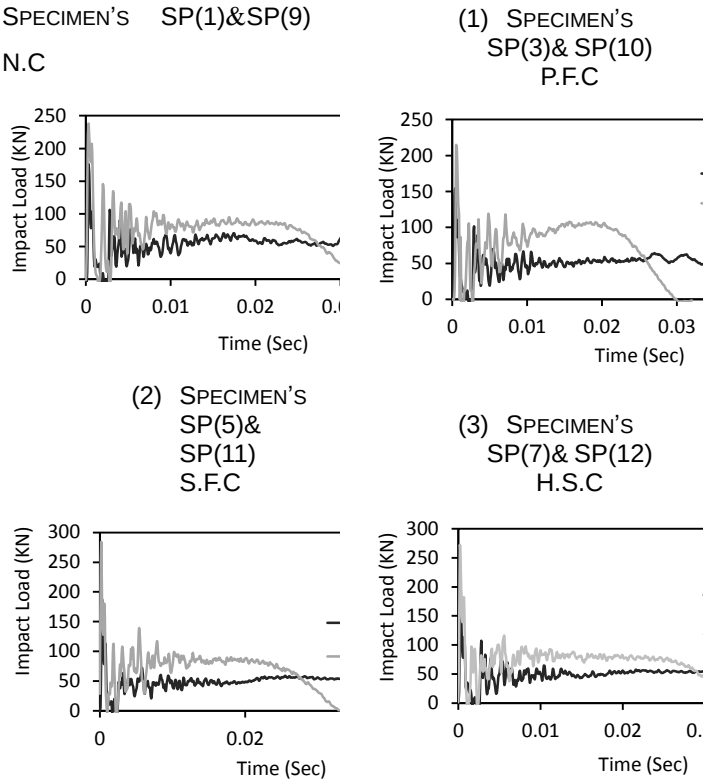

FIG. 9. *THE IMPACT VS TIME GRAPH FOR ALL SPECIMEN'S*

. $P_{k,e}$and $P_{s,e}$ are listed in

Material PROPERTIES

A locally supplied Materials were used in this study such as mild steel for tube, cement, aggregate, steel fibers, and propylene fiber as shown in Fig. 3***FIG. 3***. These materials were tested in accordance with the relevant EN and BS standards. Ordinary Portland cement CEM I/42.5N complying with the requirements of British Standard BS EN 197-1 [15] was used in the preparation of the concrete mix. Normal coarse aggregate(NA) was used with maximum size of 10 mm, graded according to the British Standard BS 882 [16] This size was selected in proportion with the specimen's diameter. Normal silicious sand was used as fine aggregate in the concrete mix. The concrete was poured in layers and compacted with vibrator in the steel tube. The mean cube compressive strength of theN.C, PP.C, and SF.C concrete was designed with approximately 45 MPa at 28-day. While, for HS.C was approximately 70 MPa. The concrete mixing, pouring, and curing, as well as theconcretes cubes and cylinders used to obtain the cube's compressive strength (Fcu) and elastic modulus (Ec) are shown in Fig. 4. A standard tensile coupon test was conducted on three samples from the two types of steel tube with the standard dimensions. The average values of

the yield strength, ultimate strength and the elongation are 326N/mm^2, 460 N/mm^2, 23% respectively. The modulus of elasticity (Es) for specimens is 2.01×10^5 N/mm^2.

TABLE 1. The results show that, The least value of $P_{k.e}$was recorded for the polypropylene fiber concrete specimens SP(3) & SP(11) with maximum value of 214 kN& 154 kN then for normal concrete specimens SP(1) & SP(9) with nearly 11% increase in maximum value of $P_{k.e}$to reach 237kN& 174kN. While, the maximum value for $P_{k.e}$was recorded for the steel fiber concrete SP(5) & SP(11), and high strength concrete SP(7) & SP(12) with nearly 25% increase in maximum value of $P_{k.e}$.

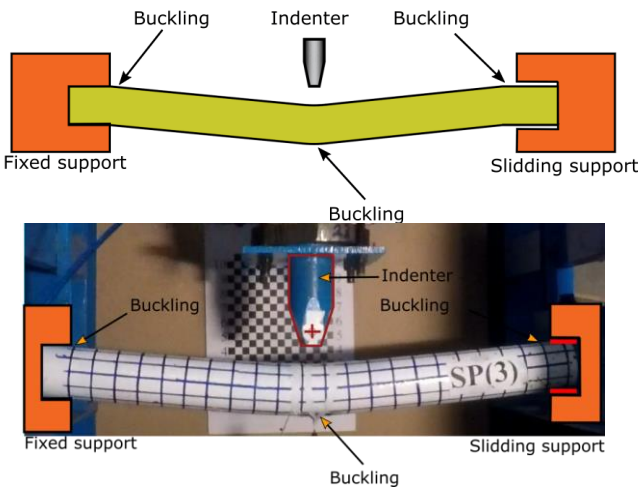

FIG. 5. *FAILURE PATTERN OF THE SPECIMENS*

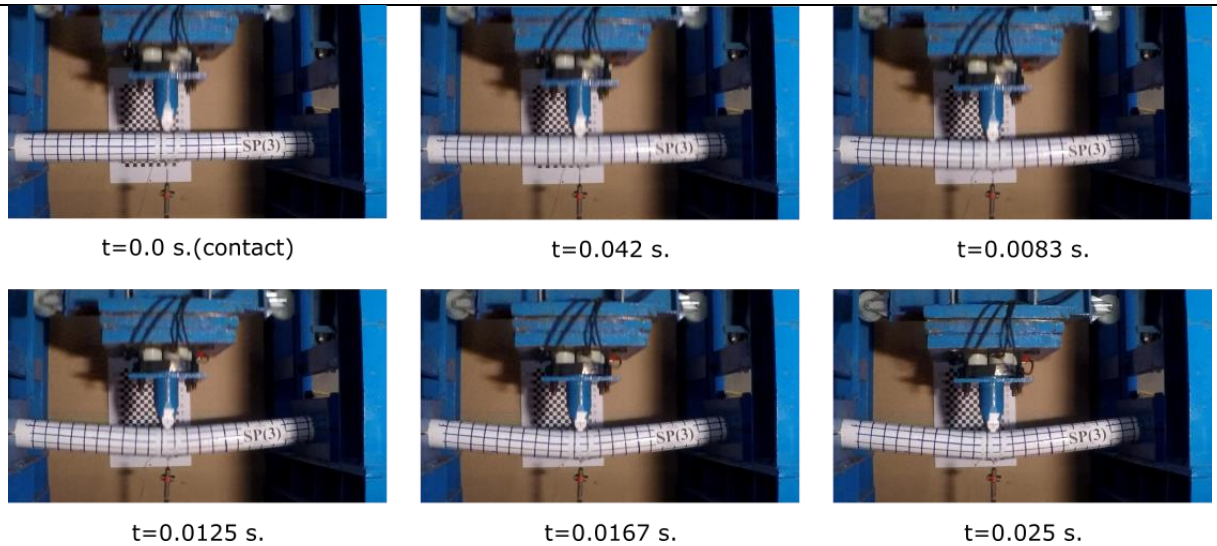

FIG. 6. THE DISPLACEMENT (U) PROGRESS OF SPECIMEN SP(3).

The plateau value of impact load ($P_{s,e}$) for all specimens was ranged between 79 KN and 96 KN for group (I) and ranged between 52 KN and 57 KN for group (II) . The largest value for the plateau of impact load was recorded for the polypropylene fiber concrete specimens SP(3) in group (I), and for the normal concrete in group (II). The impact vs time graphs for all specimens are shown in Fig. 9. The time histories of mid-span displacement (u_m) for all specimens are shown inFig. 10. The maximum dynamic experimental displacement ($u_{mm,e}$) at the mid-span is listed in

Material PROPERTIES

A locally supplied Materials were used in this study such as mild steel for tube, cement, aggregate, steel fibers, and propylene fiber as shown in Fig. 3***FIG. 3***. These materials were tested in accordance with the relevant EN and BS standards. Ordinary Portland cement CEM I/42.5N complying with the requirements of British Standard BS EN 197-1 [15] was used in the preparation of the concrete mix. Normal coarse aggregate(NA) was used with maximum size of 10 mm, graded according to the British Standard BS 882 [16] This size was selected in proportion with the specimen's diameter. Normal silicious sand was used as fine aggregate in the concrete mix. The concrete was poured in layers and compacted with vibrator in the steel tube. The mean cube compressive strength of theN.C, PP.C, and SF.C concrete was designed with approximately 45 MPa at 28-day. While, for HS.C was approximately 70

MPa. The concrete mixing, pouring, and curing, as well as theconcretes cubes and cylinders used to obtain the cube's compressive strength (Fcu) and elastic modulus (Ec) are shown in Fig. 4. A standard tensile coupon test was conducted on three samples from the two types of steel tube with the standard dimensions. The average values of the yield strength, ultimate strength and the elongation are 326N/mm^2, 460 N/mm^2, 23% respectively. The modulus of elasticity (Es) for specimens is 2.01×10^5 N/mm^2.

TABLE 1. It can be observed from group (I) that, the polypropylene fiber concrete specimens SP(3) had the least displacement value of 59 mm. While the displacement of other specimens ranged between 62 to 65 mm. Also in group (II), the least value of ($u_{mm,e}$) is recorded in the normal concrete SP(10) and polypropylene fiber concrete specimens SP(12). The maximum dynamic experimental displacement ($u_{mm,e}$) was recorded for the high strength concrete specimens SP(7) & SP(11), and for the steel fiber concrete specimens SP(5) & SP(12). The concrete strength had no improvement effect on the ($u_{mm,e}$). The calculation method of the total energy, the absorbed energy, and the recovery energy are illustrated in **Error! Reference source not found.**. The least value of the total energy (W) was recorded for polypropylene fiber concrete specimens SP(3) & SP(10). The normal, and high strength concrete specimens SP(1) & SP(7) & SP(9) & SP(12) had nearly the same total impact energy (W). The largest value of total impact energy (W) was recorded for the steel fiber concrete specimens SP(5) & SP(11). On contrast in group (I), the largest value of recovery energy was recorded for polypropylene fiber concrete specimens, then for normal, and high strength concrete specimens, then for the steel fiber concrete specimens.

FOR THE SPECIMENS.

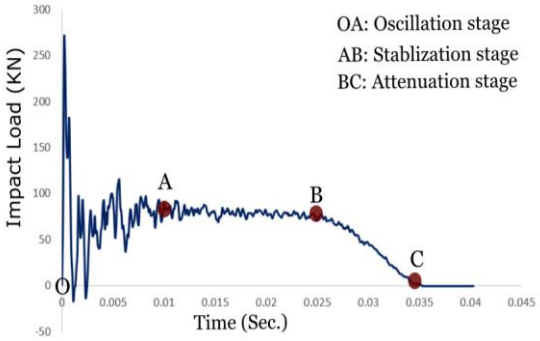

FIG. 7. TYPICAL TIME HISTORY OF IMPACT LOADS.

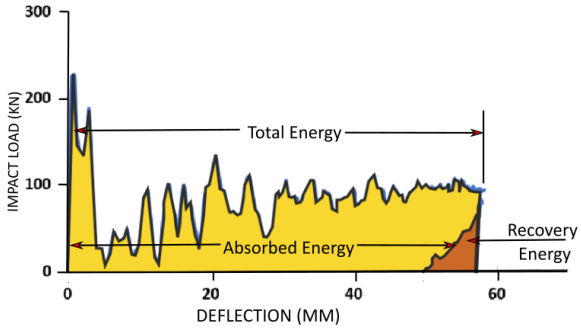

***FIG. 8**. THE TOTAL AND ABSORBED ENERGY CALCULATION*

(4) SPECIMEN'S SP(1)&SP(9) N.C

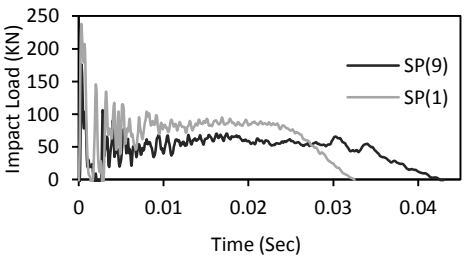

(6) SPECIMEN'S SP(5)& SP(11) S.F.C

(5) SPECIMEN'S SP(3)& SP(10) P.F.C

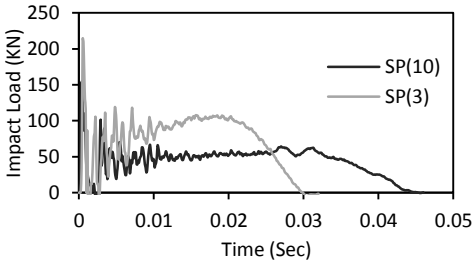

(7) SPECIMEN'S SP(7)& SP(12) H.S.C

FIG. 9. *THE IMPACT VS TIME GRAPH FOR ALL SPECIMEN'S*

(1) SPECIMEN'S SP(1)&SP(9) N.C

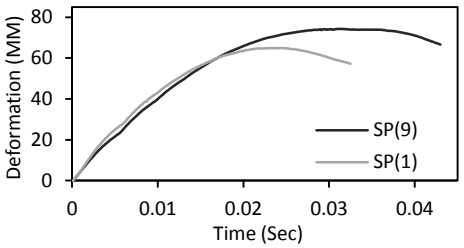

(2) SPECIMEN'S SP(3)& SP(10) P.F.C

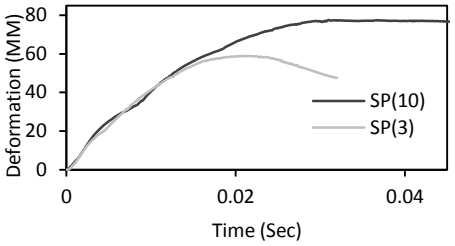

(3) SPECIMEN'S SP(5)& SP(11) S.F.C

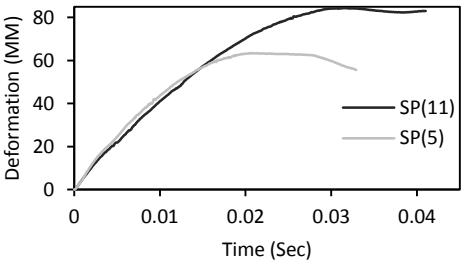

(4) SPECIMEN'S SP(7)& SP(12) H.S.C

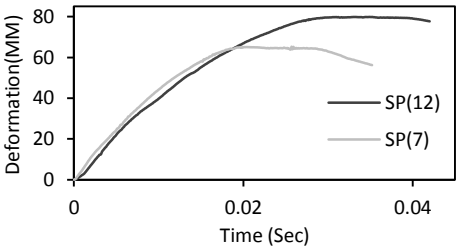

FIG. 10. THE DEFLECTION VS TIME GRAPH FORALL SPECIMEN'S

(1) SPECIMEN'S SP(1)&SP(9) N.C

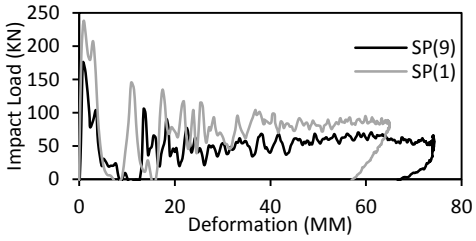

(2) SPECIMEN'S SP(3)& SP(10) P.F.C

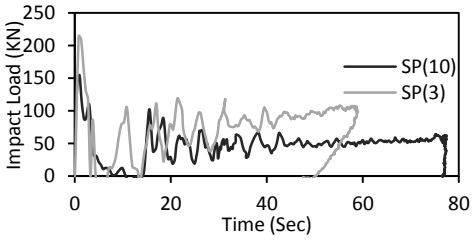

(3) SPECIMEN'S SP(5)& SP(11) S.F.C

(4) SPECIMEN'S SP(7)& SP(12) H.S.C

FIG. 11. IMPACT FORCE VS DEFLECTION GRAPH FOR ALL SPECIMENS.

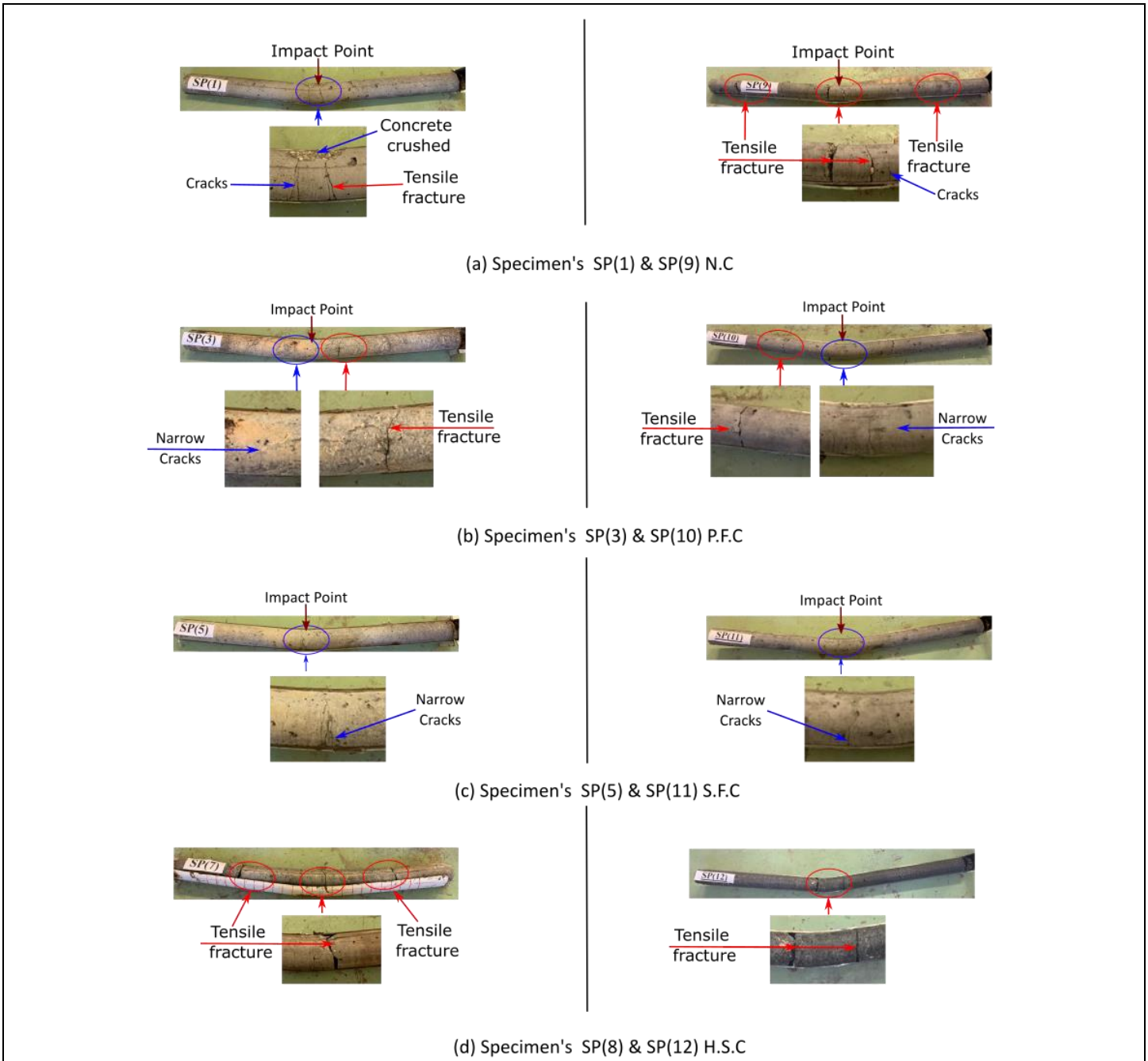

FIG. 12. FAILURE PATTERN OF THE SPECIMENS.

The failure patterns for all specimens are represented in Fig. 12. *FAILURE PATTERN OF THE SPECIMENS.*, which show

buckling of the steel tube on both sides of the impact location and crack propagation in concrete core and/or concrete core tensile fracture. Wide crackswere observed on the concrete core at the tension zone near the impact location for specimens SP(1) & SP(9) of normal concrete. Moreover, a tensile fracture on the concrete core was observed near the impact area and/or along the flat part between the mid span and the support Fig. 12(a). while, For specimens SP (7) &SP(12) of high strength concrete, a fracture of the concrete core occurred near the mid span and along the flat part Fig. 12(d). In specimens SP (3) &SP(10) of polypropylene fiber concrete, a fracture occurred in the concrete core near mid-span with narrow cracks Fig. 12(b) . In the contrast, in specimens SP (5) &SP(11) of steel fiber concrete, a narrow cracks occurred on the concrete core at the tension zone of the mid-span without any fracture observed Fig. 12(c).

4 FINITE ELEMENT ANALYSIS (FEA) MODEL

4.1 DESCRIPTION OF THE FINITE ELEMENT ANALYSIS (FEA) MODEL

A nonlinearfinite element analysis (FEA) model was establishedusing the ABAQUS/Explicit module (Hibbitt et al., 2005 [17]) tounderstandthe performance of CFST elements under lateral impact. To simulate the exact experimental conditions, the components of impact test including the steel tube, the concrete core, the hammer, as well as the interactions between concrete and steelwere all simulated in the FEA model. In addition, the boundary conditions, and the concrete core crushing criteria after impact were considered. The damping forces were not considered due to their insignificant effects during impact and reduction effect on the computational efficiency. The steel tube and the core concrete were modeled by using 8-node brick elements with reduced integration (C3D8R), while the hammer was simplified to a rigid shell surface in the same dimensions (30 x 80 mm) as the contact surface of the indenter especially, it remained almost unchanged during the impact test. The drop weight mass and the initial impact velocity were assigned to a reference point in the middle surface of the rigid shell to attain the same impact energy during all impact tests. Fig. 13shows a schematic view of the FEA model of concrete encased CFST member with circular section. A mesh convergence study was performed to identify an appropriate mesh density to ensure the simulating efficiency and achieve reliable results. Different kinds of element sizes varies between 10 and 25mm were studied to choose the suitable mesh size for the concrete core and the steel tube. A dense mesh of size 10mm × 25mm was used in the mid-span of the specimen to capture the large deformation, especially the local buckling. Whereas in the other region of specimen a medium mesh density of size of 22 mm × 25 mm was adopted. Stiffness-type hourglasscontrol was considered in the model to eliminate the zero energy modes.

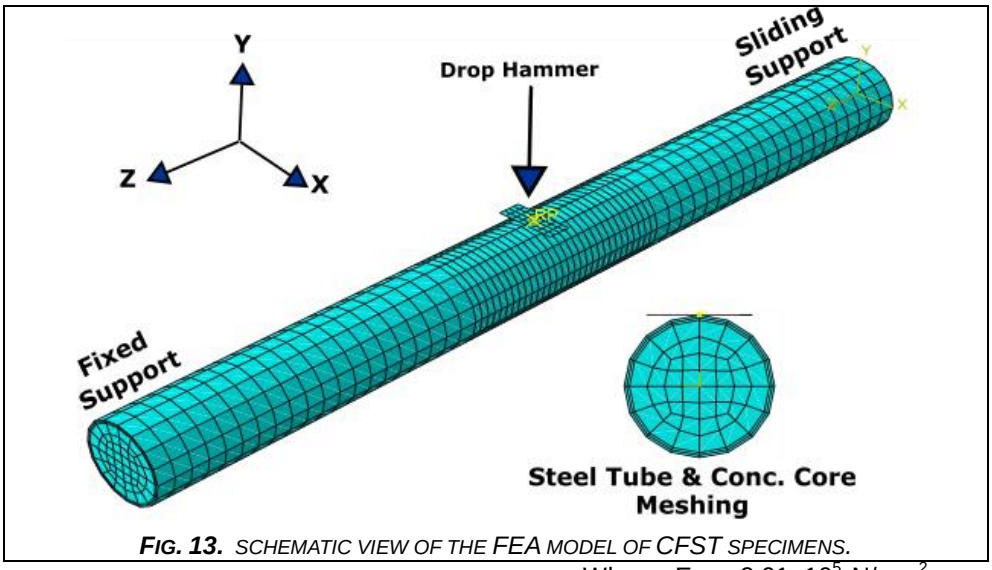

FIG. 13. *SCHEMATIC VIEW OF THE FEA MODEL OF CFST SPECIMENS.*

4.2 MATERIALS

4.2.1 Steel

Five-stage stress–strain model proposed by Han et al. [18] was used to simulate The mild steel material as shown in Fig. 14.Detailed expressions are given in Pan (1988) as:

$\sigma = E_s \cdot \varepsilon$ for $\varepsilon \le \varepsilon_1$ (1)

$\sigma = -A \cdot \varepsilon^2 + B \cdot \varepsilon + C$ for $\varepsilon_1 \le \varepsilon \le 1.5\varepsilon_1$ (2)

$\sigma = f_{sy}$ for $1.5\varepsilon_1 \le \varepsilon \le 15\varepsilon_1$ (3)

$\sigma = f_{sy} \cdot \left[1 + 0.6 \cdot \frac{\varepsilon - 150\,\varepsilon_1}{135\varepsilon_1}\right]$ for $15\varepsilon_1 \le \varepsilon \le 150\varepsilon_1$ (4)

$\sigma = 1.6 \cdot f_{sy}$ for $\varepsilon > 150\varepsilon_1$ (5)

Where, Es = 2.01×10^5 N/mm^2, $\varepsilon_1 = 0.8 \cdot f_{sy}$ (the yielding strength of the steel).

Yield and ultimate strength of steel increase during impact loading with the increase of strain rate [19]. Cowper–Symonds model gives equation to calculate the yield strength of steel under different strain rates as shown in (6.The confinement factor ξ was introduced by Han et al. (2001) [18] to quantify the “composite action” of CFST and its expressed as expressed in the following **Error! Reference source not found.**.

$$f_y^d / f_y = 1 + (\dot{\varepsilon} / D)^{1/p} \quad (6)$$

f_y is the yield strength of steel tube and f_y^d is the yield strength of steel under strain rate $\dot{\varepsilon}$.The values of D= 6844 s^{-1} andp = 3.91 [20].

$$\xi = \frac{A_S F_y}{A_C F_{ck}} = \alpha \frac{F_y}{F_{ck}} \quad (7)$$

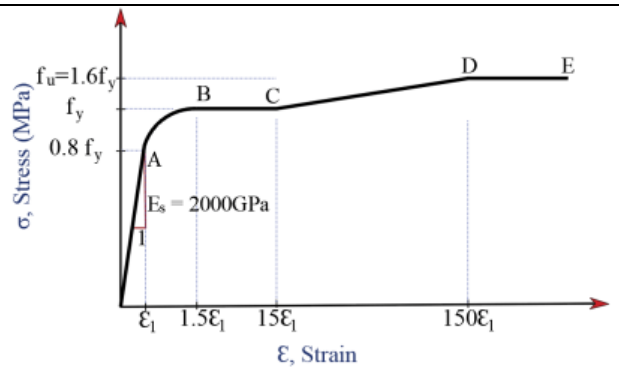

FIG. 14. *THE STEEL FIVE-STAGE STRESS–STRAIN MODEL PROPOSED BY HAN ET AL. (2001)[18]*

where F_y is the yield strength of steel, F_{ck} is the characteristic concrete strength which equal to 0.67 of the cube strengths of normal concrete, As is the steel tube cross-sectional area, Ac is the concrete core cross-sectional area, and α (=A_s /A_c) is the constraining factor (ξ) was ranged between 1.12to2.3.

4.2.2 Concrete

The concrete damaged plasticity model (CDP) in ABAQUS was used to simulate the behavior of core concrete. The following value was adopted for the CDP model, ψ= 30°, e=0.1, f_{b0}/fc0 =1.16, and K_c= 2/3 where (ψ) is the dilation angle, (e) is the flow potential eccentricity, (f_{b0}/f_{c0}) is the ratio of the compressive strength under biaxial loading to uniaxial compressive strength, and (K_c) is the ratio of the second stress invariant on the tensile meridian to that on the compressive meridian [21].

In order to simulate the plastic behaviour of core concrete in CFSTs under compression, the stress–strain relations presented in Han et al. [22] was later modified by him. [3] based on a large amount of trial calculations on CFST stub column test results to suit for the FEA using ABAQUS software. The modified stress–strain model is represented by (8. The proposed concrete model considered the increase in the plasticity of the concrete core because of the passive confinement of the steel tube as shown in Fig. 17(a).

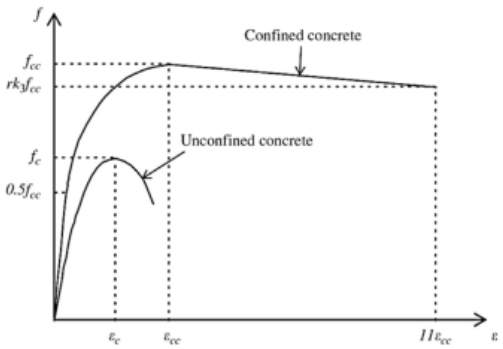

(a) RELATIONSHIP OF CONfiNED AND UNCONfiNED CONCRETE[22]

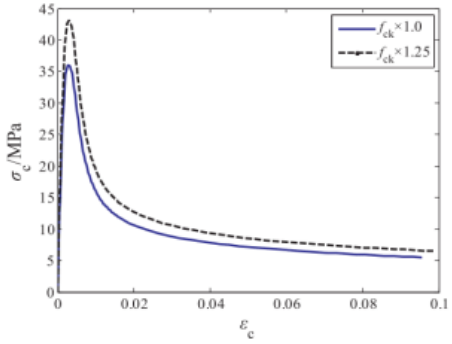

(b) CONCRETE WITH AND WITHOUT DYNAMIC INCREASE FACTOR[13].

FIG. 15. *COMPARISON BETWEEN STRESS-STRAIN CURVES OF CONFINED AND UNCONFINED CONCRETE AND THE EFFECT OF STRAIN RATE ON CONCRETE.*

$$y = \begin{cases} 2x - x^2 & (x \le 1) \\ \dfrac{x}{\beta_0 (x-1)^{\eta} + x} & (x > 1) \end{cases} \quad (8)$$

$$\text{where} x = {}^{\varepsilon}/_{\varepsilon_0}, \quad y = {}^{\sigma}/_{\sigma_o}, \quad \sigma_o = f_c' \left(\frac{N}{mm^2}\right);$$

$$\varepsilon_0 = \varepsilon_c + 800\xi^{0.2} * 10^{-6}; \; \varepsilon_c = (1300 + 12.5\, f_c') * 10^{-6}$$

$$\eta = \begin{cases} 2 & (\text{CFSTwithcircularsection}) \\ 1.6 + 1.5x & (\text{CFSTwithsquaresection}), \end{cases}$$

$$\beta_0 = \begin{cases} (2.36 * 10^{-5})^{[0.25+(\xi-0.5)^7]} (f_c')^{0.5} * 0.5 \ge 0.12 & (\text{CFSTwithcircularsection}) \\ \dfrac{(f_c')^{0.1}}{1.2\sqrt{1+\xi}} & (\text{CFSTwithsquaresection}) \end{cases}$$

The strain- curve for the steel fiber concrete are calculated based on the model proposed by Carreira and Chu [23], whose general expression is given by(9,

$$\frac{\sigma_c}{f_c} = \frac{\beta \left({}^{\varepsilon_c}/_{\varepsilon_{c,0}}\right)}{\beta - 1 + \left({}^{\varepsilon_c}/_{\varepsilon_{c,0}}\right)^{\beta}} \quad (9)$$

$$\beta = (0.0536 - 0.5754 V_f) f_c$$

$$\varepsilon_{c,0} = (0.00048 + 0.01886 V_f) \ln f_c$$

where, σ_c is the compressive stress, f_c is the compressive strength, ε_c is the strain, $\varepsilon_{c,0}$ is the peakstrain and β is the factor which considers the influence of fibers on the curve form. The parameters β and$\varepsilon_{c,0}$ can be obtained, in general, by equations that correlates these parameters to fiber volumetric fractionand/or to the compressive strength of concrete. In general, the equations of β and$\varepsilon_{c,0}$ are correlated to fiber volumetric fractionand/or to the compressive strength of concrete [24]. According to the ACI Committee 318 recommendations [25], The initial modulus of elasticity was taken as $Ec = 4730\sqrt{f_c'}$, and Poisson's ration as μc = 0.2, where f_c' was the concrete cylinder strength (in N/mm2), $f_c' = f_{ck} + 8$ [38]. $f_{ck} = 0.67\, f_{cu}$ where f_{ck}&f_{cu} are the characteristic static compressive strength, and the average measured cubic compressive strength of concrete at 28 days, respectively. The effect of impact load on the concrete strength was considered by multiplying f_{ck} by a dynamic increase factor of 1.25 [26, 27] as shown inFig. 17 (b). Moreover, the modulus of elasticity of concrete remained insensitive to the rate of loading [27] .

4.3 Boundary condition and contact

The specimen was fixed from one end while the other end was released only in the longitudinal direction. To demonstrate the contact between the steel tube inner surface and the concrete outer surface, in the normal direction, a surface-based interaction with a contact pressure model “hard contact” was used, thereby allowing the interface separation in tension without penetration of that in compression [33]. A Coulomb friction was used for the model in the tangential direction, thereby the frictional behaviour between the surfaces was specified by a friction factor equal to 0.47 according to Baltay et al. [28].

4.4 Verifications of the FEA model

The finite element analysis model was validated by comparing the tested results (including the impact process, the horizontaldisplacement, and the failure modes) with the predicted results as shown in
Fig. ***16***. The comparison between the measured and the predicted impact force (F) and the displacement vs time (t) curves for the specimens are presented inFig. 17&Fig. 18. The comparisons of impact load ($P_{k,e}$), the maximum dynamic experimental displacement ($u_{mm,e}$), and the total impact energy (W) between the experimental and predicted results are demonstratedin Table 3. It can be seen from the figures and table that, the F.E.M can predict well the deformation and impact force of the specimens. A reasonably good agreementbetween the test and F.E.M results is obtained.However, the total impact energy (W) of the F.E.M are a slightly higher than the tested results. This may contribute to the fact that, the FEAmodel cannot simulate the friction between devices, effect of air resistance, and environmental interference. Also, the F.E.M did not consider the internal cracks of the steel tube. The unloading trend of the measured impact load history in the test is slower than in the predicted one in the F.E.M. This contributes to the fact that, the expanding of crack in the steel tube would decrease the stiffness of the specimen and thus the trend of the unloading changes.

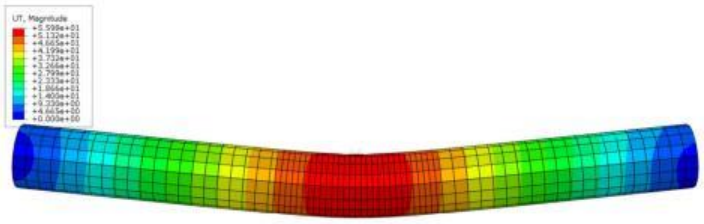

(a) F.E.M maximum dynamic displacement (umm,e) for SP(3)& SP(4)

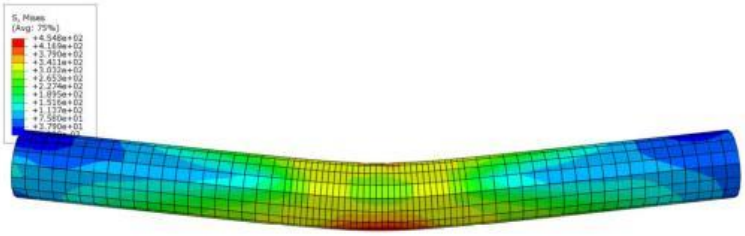

(b) F.E.M von miss stress of steel tube for SP(3)& SP(4) corresponding to maximum (umm,e)

Fig. 16. *Sample for typical failure patterns for all specimens.*

Table 3.
Information of the specimens.

SPEC. ID	Pipe Type	$P_{K.e}$(KN)		F.E.M/ Tested	$U_{mm,e}$ (mm)		F.E.M/ Tested	W (J)		F.E.M/ Tested	Concrete failure
		Tested	F.E.M		Tested	F.E.M		Tested	F.E.M		

			Pipe Clear Length =1200MM									
Group (I)	SP(1)	114.3*4	237	248	1.05	64	63	0.98	5056	5796	1.14	A
	SP(3)	114.3*4	214	234	1.09	59	56	0.95	4801	5812	1.21	B
	SP(5)	114.3*4	284	272	0.96	63	62	0.98	5135	6570	1.28	A
	SP(7)	114.3*4	268	271	1.01	65	64	0.98	4929	6423	1.30	B
Group (II)	SP(9)	89*4	177	174	0.98	74	76	1.027	3864	4561	1.18	B
	SP(10)	89*4	154	157	1.02	77	79	1.025	3665	4559	1.24	A + B
	SP(11)	89*4	187	180	0.96	84	81	0.96	3975	4539	1.14	A
	SP(12)	89*4	195	178	0.91	79	80	1.012	3741	4423	1.18	B

A: tensile cracks at tension side, B: facture of concrete core.

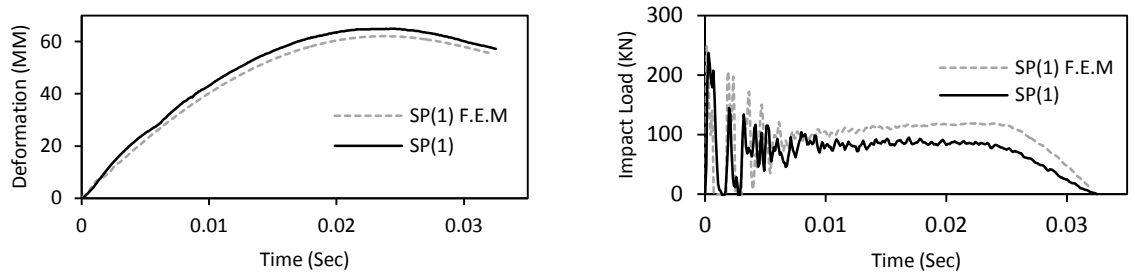

(a) SPECIMEN'S SP(1)

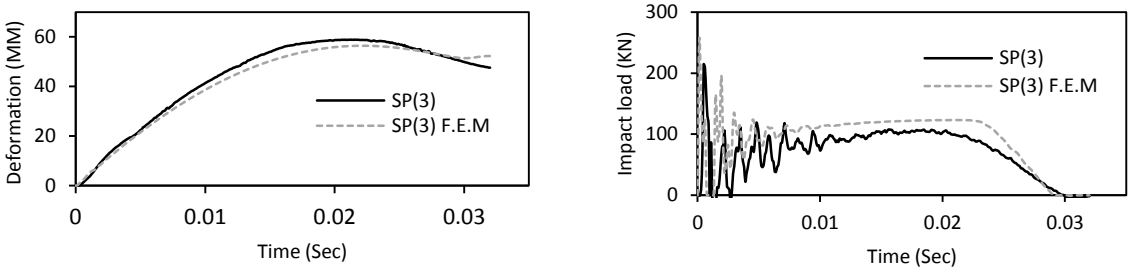

(b) SPECIMEN'S SP(3)

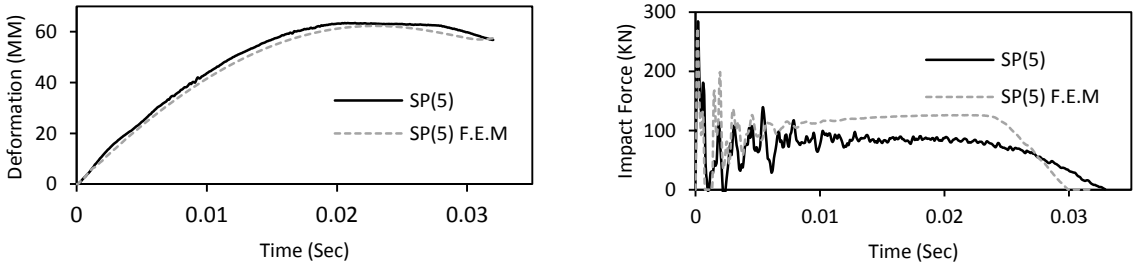

(c) SPECIMEN'S SP(5)

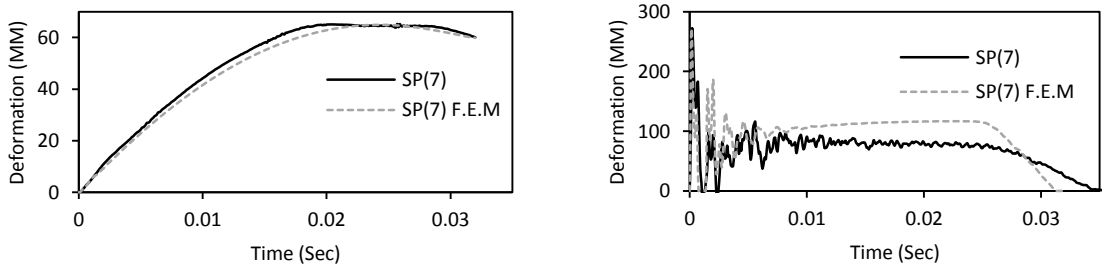

(d) SPECIMEN'S SP(7)

FIG. 17 COMPARISON BETWEEN THE F.E.M AND TESTED RESULTS FOR SPECIMEN'S SP(1 & 3 & 5 & 7)

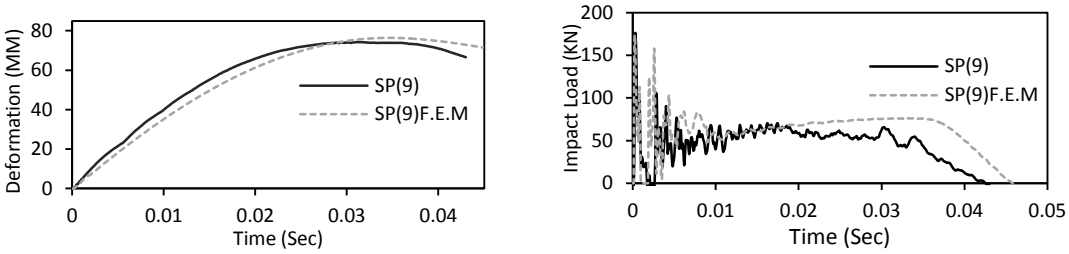

(a) SPECIMEN'S SP(9)

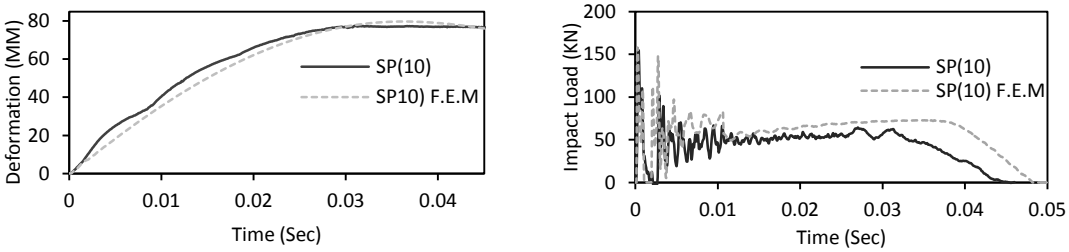

(b) SPECIMEN'S SP(10)

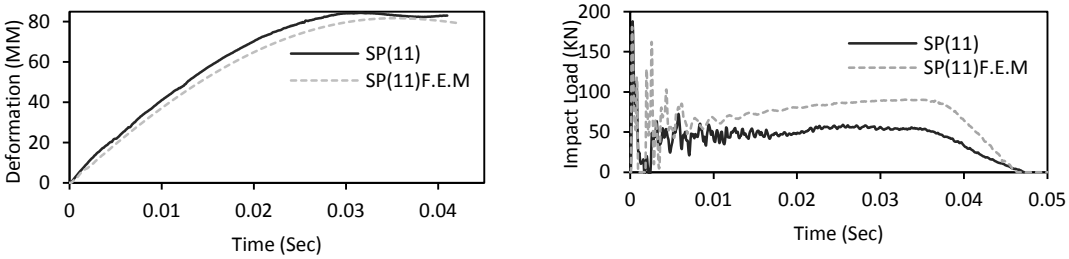

(c) SPECIMEN'S SP(11)

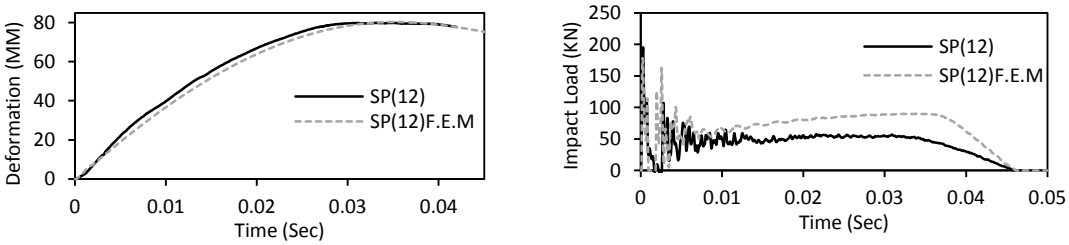

(d) SPECIMEN'S SP(12)

FIG. 18 COMPARISON BETWEEN THE F.E.M AND TESTED RESULTS FOR SPECIMEN'S SP(1 TO 4)

5 CONCLUSIONS

In this study an experimental and numerical study were conducted toinvestigate the performance of circular CFST members under lateral impact loading filled with different types of concrete (Normal concrete, Polypropylene fiber concrete, Steel fiber concrete, and High strength concrete). Based on the observations and analytical results, we can conclude that:

(a) all specimens were characterized by V-shapeFailure mode at the impacted area. the core concrete was cracked at the mid-span section and may be fractured near the impact area and along the flat part of specimen around the impact area.

(b) Polypropylene concrete specimens had the lowset value of $P_{k,e}$, $P_{s,e}$, $u_{mm,e,}$ and W than those of all other types of concrete specimens. While the maximum recovery energy $W_{Recovery}$ was recorded for the polypropylene concrete specimens in group (I).which mean that polypropylene concretecan absorb the induced energy of the impact.

(c) Normal concrete specimen in group (II) has lower value in $u_{mm,e,}$ thanPolypropylene concrete specimen. This may be due to the occurrence of a fracture on the concrete core before it reached its final deformation, such as what happened to the first group (I)

(d) High strength concrete specimens had nearly the same values of $P_{k,e}$, $P_{s,e}$, $u_{mm,e}$, and W or slightly higher than those of normal concrete except normal concrete specimens in group (II), which mean that, no benefit was gained form increasing the concrete strength. On the other hand, it may have triggered brittle failure for the concrete core.

(e) The deformations for steel fiber concrete, normal concrete, and high strength concrete specimens were nearly in the same values, however, the steel fiber concrete specimens displayed ductile behaviour with less concrete cracks.

(f) high strength concrete specimens has The lowest values of constraining factor (ξ) , which behave in the most brittle failure pattern. so, Ductility of the tested specimens increase with the constraining factor (ξ).

REFERENCES

[1] A. Seminar, "Concrete Filled Steel Tubes—A Comparison of International Codes and Practices," Innsbruck, September. Google Scholar, 1997.

[2] N. E. Shanmugam and B. Lakshmi, "State of the art report on steel–concrete composite columns," Journal of constructional steel research, vol. 57, no. 10, pp. 1041-1080, 2001.

[3] L.-H. Han, G.-H. Yao, and Z. Tao, "Performance of concrete-filled thin-walled steel tubes under pure torsion," Thin-Walled Structures, vol. 45, no. 1, pp. 24-36, 2007.

[4] U. Starossek, N. Falah, and T. Lohning, "Numerical analyses of the force transfer in concrete-filled steel tube columns," Structural engineering and mechanics: An international journal, vol. 35, no. 2, pp. 241-256, 2010.

[5] D. Lam and K. Wong, "Axial capacity of concrete filled stainless steel columns," in Structures Congress 2005: Metropolis and Beyond, 2005, pp. 1-11.

[6] S.-F. Jiang, Z.-Q. Wu, and D.-S. Niu, "Experimental study on fire-exposed rectangular concrete-filled steel tubular (CFST) columns subjected to bi-axial force and bending," Advances in Structural Engineering, vol. 13, no. 4, pp. 551-560, 2010.

[7] H. Sharma, S. Hurlebaus, and P. Gardoni, "Performance-based response evaluation of reinforced concrete columns subject to vehicle impact," International Journal of Impact Engineering, vol. 43, pp. 52-62, 2012.

[8] B. EN, "1-7 Eurocode I: actions on structures-Part 1-7. general actions—accidental actions [S]," Brussels: European Committee for Standardization, vol. 2006, pp. 53-55, 1991.

[9] M. R. Bambach, H. Jama, X.-L. Zhao, and R. Grzebieta, "Hollow and concrete filled steel hollow sections under transverse impact loads," Engineering Structures, vol. 30, pp. 2859-2870, 10/01 2008, doi: 10.1016/j.engstruct.2008.04.003.

[10] Y.-F. Yang, Z.-C. Zhang, and F. Fu, "Experimental and numerical study on square RACFST members under lateral impact loading," Journal of Constructional Steel Research, vol. 111, pp. 43-56, 2015.

[11] A. Al-Husainy, "Impact response of recycled aggregate concrete filled steel tube columns strengthened with CFRP," University of Liverpool, 2017.

[12] H. Qu, G. Li, S. Chen, J. Sun, and M. Sozen, "Analysis of Circular Concrete-Filled Steel Tube Specimen under Lateral Impact," Advances in Structural Engineering, vol. 14, pp. 941-952, 10/01 2011, doi: 10.1260/1369-4332.14.5.941.

[13] A.-Z. Zhu, W. Xu, K. Gao, H.-B. Ge, and J.-H. Zhu, "Lateral impact response of rectangular hollow and partially concrete-filled steel tubular columns," Thin-Walled Structures, vol. 130, pp. 114-131, 2018.

[14] Y. Deng, C. Tuan, and Y. Xiao, "Flexural Behavior of Concrete-Filled Circular Steel Tubes under High-Strain Rate Impact Loading," Journal of Structural Engineering, vol. 138, pp. 449-456, 03/01 2012, doi: 10.1061/(ASCE)ST.1943-541X.0000464.

[15] B. En, "197-1: 2011," Cement, Composition, Specifications and Conformity Criteria for Common Cements. London, England: British Standard Institution (BSI), 2011.

[16] A. No, "Specification for aggregates from natural sources for concrete," ed: BS, 1992.

[17] U. m. Abaqus and S. U. s. Manual, "Hibbitt, Karlsson, and Sorensen," Inc V5, vol. 8, 2005.

[18] L.-H. Han, X.-L. Zhao, and Z. Tao, "Tests and mechanics model for concrete-filled SHS stub columns, columns and beam-columns," Steel and Composite Structures, vol. 1, no. 1, pp. 51-74, 2001.

[19] N. Jones, Structural impact. Cambridge university press, 2011.

[20] W. Abramowicz and N. Jones, "Dynamic axial crushing of square tubes," International Journal of Impact Engineering, vol. 2, no. 2, pp. 179-208, 1984.

[21] Z. Tao, Z.-B. Wang, and Q. Yu, "Finite element modelling of concrete-filled steel stub columns under axial compression," Journal of constructional steel research, vol. 89, pp. 121-131, 2013.

[22] L.-H. Han, G.-H. Yao, and X.-L. Zhao, "Tests and calculations for hollow structural steel (HSS) stub columns filled with self-consolidating concrete (SCC)," Journal of Constructional Steel Research, vol. 61, pp. 1241-1269, 09/01 2005, doi: 10.1016/j.jcsr.2005.01.004.

[23] D. Carreira and K.-H. Chu, "Stress-strain relationship for plain concrete in compression," Journal of the American Concrete Institute, vol. 82, pp. 797-804, 11/01 1985.
[24] L. Oliveira Júnior et al., "Stress-strain curves for steel fiber-reinforced concrete in compression," Matéria (Rio de Janeiro), vol. 15, pp. 260-266, 01/01 2010, doi: 10.1590/S1517-70762010000200025.
[25] A. Committee, "Building code requirements for structural concrete:(ACI 318-02) and commentary (ACI 318R-02)," 2002: American Concrete Institute.
[26] M. Yousuf, B. Uy, Z. Tao, A. Remennikov, and J. R. Liew, "Impact behaviour of pre-compressed hollow and concrete filled mild and stainless steel columns," Journal of Constructional Steel Research, vol. 96, pp. 54-68, 2014.
[27] G. Mays, P. D. Smith, and P. D. Smith, Blast effects on buildings: Design of buildings to optimize resistance to blast loading. Thomas Telford, 1995.
[28] P. Baltay and A. Gjelsvik, "Coefficient of friction for steel on concrete at high normal stress," Journal of Materials in Civil Engineering, vol. 2, no. 1, pp. 46-49, 1990.